Archives of Oral Biology 157 (2024) 105851

Contents lists available at ScienceDirect

Archives of Oral Biology

journal homepage: www.elsevier.com/locate/archoralbio

High glucose levels delay the senescence of stem cells from human exfoliated deciduous teeth by suppressing autophagy

Jinjin Lu [a], Lixin Zhang [a], Ningxin Zhu [a], Dan Wang [a], Fei Xie [a], Man Qin [a], Yuanyuan Wang [a,*]

[a] Department of Pediatric Dentistry, School and Hospital of Stomatology, Peking University, Beijing, China

ARTICLE INFO

Keywords:
Glucose
Human bone marrow-derived mesenchymal stem cells
Human exfoliated deciduous teeth stem cells
Autophagy

ABSTRACT

Objective: In this study, we aimed to investigate the effects of varying glucose concentrations on the proliferation and senescence of stem cells from human exfoliated deciduous teeth (SHED) compared to human bone marrow-derived mesenchymal stem cells (hBMSC), and preliminarily clarify the difference of glucose metabolism between SHED and hBMSC.

Design: We cultured SHED and hBMSC in the presence of increasing glucose concentrations to study the role of glucose in cell viability, proliferation, and senescence. Gene expression related to the stemness of mesenchymal stem cells was evaluated using real-time quantitative reverse transcription-polymerase chain reaction. In addition, glucose consumption, lactic acid production, oxidative phosphorylation, and glycolysis were measured to analyze glucose metabolism and expression of autophagy-related markers, including microtubule-associated proteins 1 A/1B light chain 3 B and p62.

Results: While a high glucose level (4.5 g/L) promoted the proliferation of both SHED and hBMSC, it delayed senescence in SHED via autophagy inhibition but accelerated hBMSC senescence. In contrast to that in hBMSC, glycolysis in SHED was enhanced under the high-glucose culture condition.

Conclusions: The glycometabolism of SHED and hBMSC differed, and a high glucose culture medium was more favorable for SHED.

1. Introduction

Stem cells from human exfoliated deciduous teeth (SHED) offer strong potential for tissue engineering. This is due to their remarkable proliferative capacity, cell stemness, multilineage differentiation capacity, and ease of acquisition with few ethical concerns (Kunimatsu et al., 2018; Miura et al., 2003; Zhang et al., 2016). Different in vivo mesenchymal stem cell (MSC) niches and in vitro microenvironments guide MSC dynamics (Sakaguchi, Sekiya, Yagishita, & Muneta, 2005; Yoshimura et al., 2007).

Glucose metabolism is the primary driver of microenvironmental changes affecting cell growth, proliferation, and bioprocess product quality. The influence of glucose on the behavior of different types of mesenchymal stem cells (MSC) appears to vary. In the case of human bone marrow-derived mesenchymal stem cells (hBMSC) for example, a high glucose level (4.5 g/L) both promotes cell proliferation by activating the MAPK and PI3K/Akt signaling pathways (Ryu, Lee, Yun, & Han, 2010) and increases cell senescence by promoting autophagy (Chang, Hsu, & Wu, 2015). However, high glucose levels do not affect the proliferation of human dental pulp stem cells (Kichenbrand, Grossin, Menu, & Moby, 2020) but instead promote their aging through the Wnt/β-catenin signaling pathway (Asghari, Nasoohi, & Hodjat, 2021). The influence of glucose on SHED growth, apoptosis, and senescence remains to be elucidated.

Therefore, we investigated the effects of varying glucose concentrations on the proliferation and senescence of SHED compared with hBMSC. In addition, we explored the intrinsic mechanism by which glucose alters the cell dynamics of SHED from a glycometabolic perspective.

Abbreviations: SHED, stem cells from human exfoliated deciduous teeth; MSC, mesenchymal stem cells; hBMSC, human bone marrow-derived mesenchymal stem cells; LC3B, microtubule-associated proteins 1 A/1B light chain 3 B; DMEM, Dulbecco's modified Eagle's medium; PBS, phosphate-buffered saline; RT-qPCR, reverse transcription quantitative polymerase chain reaction; GAPDH, glyceraldehyde 3-phosphate dehydrogenase; AMPK, adenosine 5′-monophosphate protein kinase alpha 1; OXPHOS, oxidative phosphorylation; Rot/AA, rotenone and antimycin.

* Corresponding author.
E-mail address: cwyyd@126.com (Y. Wang).

https://doi.org/10.1016/j.archoralbio.2023.105851
Received 23 August 2023; Received in revised form 29 October 2023; Accepted 14 November 2023
Available online 17 November 2023

2. Materials and methods

2.1. Cell culture

SHED from children (aged 5–7 years) were provided by the Oral Stem Cell Bank (Beijing Tason Biotech Co., Ltd., Beijing, China), and three SHED samples were included. hBMSC were purchased from Procell Life Science & Technology Co., Ltd. (Wuhan, China). Both cell types were cultured in a proliferation medium containing Dulbecco's Modified Eagle's Medium (DMEM; Procell) with 1 g/L glucose and 10% fetal bovine serum (Procell) at 37 °C in 5% CO_2 and 95% humidity. After reaching 80–90% confluence, cells in passages 3–5 were harvested using 0.05% trypsin-ethylenediaminetetraacetic acid (EDTA) (Solarbio, Beijing, China) and subcultured for further experiments. Based on previous studies (Asghari et al., 2021; Chang et al., 2015; Kichenbrand et al., 2020; Kim et al., 2012), we chose glucose concentrations of either 1, 4.5, or 0.4, 0.6, and 0.8 g/L, allowing us to mimic physiological, hyperglycemic, and hypoglycemic conditions, respectively. Glucose concentrations in DMEM were either 0, 1 (normal), or 4.5 g/L (high). Low glucose media (0.4, 0.6, or 0.8 g/L) were prepared by mixing 0 and 1.0 g/L DMEM at the appropriate ratio.

2.2. Proliferation assay

Cell counting kit-8 (Yeasen, Shanghai, China) assays were used to detect the effect of glucose concentration on cell proliferation. Cell aliquots (200 μL; 1×10^4 cells/mL) were added to a 96-well plate, followed by the addition of glucose to final concentrations of 0.4, 0.6, 0.8, 1.0, or 4.5 g/L. Cells were incubated for 3, 7, or 14 d at 37 °C in a humidified 5% CO_2 atmosphere. The medium was replaced with 180 μL of phosphate-buffered saline (PBS) (Gibco/Thermo Fisher, Waltham, MA, USA) and 20 μL of cell counting kit-8 solution. Following this, cells were incubated for another 1 h. Absorbance was measured at 450 nm using a microplate reader (ELx808, BioTek/Agilent, Santa Clara, CA, USA). The normal glucose group (1 g/L) was used as a control to ascertain relative cell proliferation.

2.3. Apoptosis assay

Apoptosis was measured using an annexin V-FITC/PI kit (Solarbio). Specifically, SHED were seeded in six-well plates (3×10^5 cells/well); 1×10^5 cells were collected from the glucose groups 24 and 48 h later, washed twice with PBS, and resuspended in 100 μL of binding buffer. Annexin V-APC (5 μL) and propidium iodide solution (5 μL) were added and the cells were incubated for 15 min at room temperature (25 ℃). Within 1 h of this, followed by flow cytometry (NovoCyte, Agilent Technologies, Santa Clara, CA, USA).

2.4. β-galactosidase activity staining

Cells were seeded in six-well plates at 3×10^4 cells/well and cultured in a medium containing a specific glucose concentration at 37 °C and 5% CO_2 throughout their proliferative life span (14 d). Senescence-associated β-galactosidase (SA-β-Gal) activity staining was performed using the fixation buffer and staining solution provided in the kit (Solarbio), as per the manufacturer's instructions. The culture medium was then aspirated, and the cells were washed twice with PBS (Gibco/Thermo Fisher). Following this, cells were treated with fixation buffer (1 mL/well) for 15 min and washed three times with PBS (1 mL/well). Cells were then treated with staining solution (1 mL/well) and incubated overnight at 37 °C (without CO_2). Digital images of SA-β-Gal staining were captured using a light microscope (IX73 Olympus, Tokyo, Japan), after which cells were counted and the percentage of β-galactosidase-positive cells calculated.

2.5. RNA isolation and reverse transcription quantitative polymerase chain reaction

Collected cell samples were washed twice with PBS on ice. Total RNA was extracted using TRIzol reagent (Sigma-Aldrich, St. Louis, MO, USA), as per the manufacturer's protocol. DNase I-treated RNA (1 μg) was used for reverse transcription with a Hieff First Strand cDNA Synthesis Super Mix for reverse transcription quantitative polymerase chain reaction (RT-qPCR) kit (Yeasen). RT-qPCR was then performed using a Hieff qPCR SYBR Green Master Mix kit (Yeasen). The expression of each target gene was normalized to that of the housekeeping gene glyceraldehyde 3-phosphate dehydrogenase (*GAPDH)*, and fold differences were calculated using the $2^{-\Delta\Delta CT}$ method. The DNA primers for markers related to stem cell characteristics *CD73*, *CD146,* and *CD90* were synthesized by Sangon Biotech (Shanghai, China). The following primer sequences were used: *GAPDH* (forward: 5′ GTCTCCTCTGACTTCAACAGCG 3′, reverse: 5′ ACCACCCTGTTGCTGTAGCCAA3′); *CD73* (forward: 5′ AGTCCACTGGAGAGTTCCTGCA 3′, reverse: 5′ TGAGAGGGTCATAACTGGGCAC 3′); *CD90* (forward: GAAGGTCCTCTACTTATCCGCC;.

reverse: TGATGCCCTCACACTTGACCAG) *CD146* (forward: 5′ ATCGCTGCTGAGTGAACCACAG 3′; reverse: 5′ CTACTCTCTGCCTC ACAGGTCA3′).

2.6. Glucose and lactic acid measurement

Changes in glucose consumption and lactic acid production in normal and high-glucose media were determined using spectrophotometry after 6, 12, 24 and 48 h of cultivation, using commercial glucose (Jiancheng Bioengineering Institute, Jiangsu, China) and lactic acid (Jiancheng) assay kits. Measurements were performed according to the manufacturer's instructions and the results were standardized according to the number of cells in each experiment.

2.7. Western blotting

Cell samples were harvested, washed twice with PBS on ice, then lysed in lysis buffer containing a protease inhibitor cocktail (Solarbio). The proteins were separated on 10% sodium dodecyl sulfate-polyacrylamide gels (Bioss, Beijing, China) and transferred to polyvinylidene difluoride membranes (Thermo Fisher). Membranes were blocked with 5% bovine serum albumin for 2 h and then incubated overnight with primary antibodies against microtubule-associated proteins 1 A/1B light chain 3 B (LC3B; Proteintech, Wuhan, China), p62 (Proteintech), p21 (Proteintech), adenosine 5′-monophosphate protein kinase alpha 1 (AMPK; Zenbio, Chengdu China), and phospho-AMPK alpha 1 (p-AMPK; Zenbio) at dilutions of 1:1000, and GAPDH (Proteintech) at a dilution of 1:3000. Subsequently, the membranes were incubated with secondary antibodies (Proteintech) at a dilution of 1:3000 for 1 h and the blotted bands were visualized using enhanced chemiluminescence (Yeasen).

2.8. Metabolic flux

The rate of oxidative phosphorylation (OXPHOS) and glycolysis in hBMSC and SHED were monitored using a seahorse metabolic flux analyzer (Agilent), XF cell mito stress test kit (OXPHOS: Agilent), and XF glycolytic rate assay kit (Glycolysis: Agilent). SHED and hBMSC were incubated on XF24 culture microplates with normal or high glucose concentrations for 24 h. Sensor cartridges were hydrated in XF calibrant at 37 °C overnight. One hour prior to conducting the bioenergetic assays, the culture medium was replaced with unbuffered DMEM (pH 7.4) supplemented with 4 mM L-glutamine. The OXPHOS rate was measured In accordance with the Mito Stress Test, including oligomycin (1.5 μM), carbonyl cyanide-4-(trifluoromethoxy) phenylhydrazone (FCCP; 1.5 μM), rotenone and antimycin (Rot/AA; 0.5 μM each). The glycolytic rate was measured using a glycolytic rate assay kit; specifically Rot/AA (0.5

μM each); 2-deoxy-D-glucose (2-DG; 50 mM).

2.9. Statistical analysis

Data are presented as the means ± standard deviations. Student's t test was used to analyze the significance of differences between two groups. For comparisons among more than two groups, one-way ANOVA was used if the data passed the normality tests and was followed by Tukey's multiple comparison test for all pairs of groups. GraphPad Prism software version 9.4.1 (GraphPad Software Inc., La Jolla, CA, USA). was used for data management and statistical analyses. Values of $p < 0.05$ * , $p < 0.01$ * *, $p < 0.001$ * ** were considered significant.

3. Results

3.1. High glucose concentration promotes proliferation and inhibits apoptosis of SHED and hBMSC

Glucose concentration affected proliferation and apoptosis of SHED (Fig. 1A and C) and hBMSC (Fig. 1B and D). A high glucose concentration (4.5 g/L) significantly increased proliferation of SHED and hBMSC after 14 d of culture. With increasing culture time (7 d and 14 d), compared with normal glucose concentration respectively, low glucose concentrations (0.4 and 0.6 g/L) inhibited both SHED and hBMSC proliferation (Fig. 1A and B). However, a high glucose concentration significantly inhibited SHED apoptosis ($p = 0.0051$) after 24 h of culture and hBMSC apoptosis ($p = 0.0405$) after 48 h compared with the normal glucose concentration, respectively.

3.2. High glucose concentration inhibits senescence in SHED but promotes it in hBMSC

The effects of glucose concentrations on the senescence of SHED (Fig. 2A) and hBMSC (Fig. 2B) were determined using SA-β-Gal staining. Compared with the normal glucose group, the number of β-galactosidase-positive SHED in the high-glucose group was significantly lower (Fig. 1A: 0.0055); in contrast, the number of β-galactosidase-positive hBMSC in the high-glucose group was higher (Fig. 2B: $p = 0.0001$). Compared with the normal glucose group, no significant differences were observed in SHED senescence at a glucose concentration of 0.8 g/L, and low glucose concentrations (0.4 and 0.6 g/L) increased senescence in SHED but did not affect hBMSC senescence.

The expression of *CD73*, *CD90,* and *CD146* associated with MSC biomarkers in SHED (Fig. 2C) and hBMSC (Fig. 2D) was evaluated using RT-qPCR. This revealed that the high glucose concentration increased the expression of all analyzed genes in SHED, when compared to normal glucose group. Conversely, the high glucose concentration inhibited the expression of these genes in hBMSC at 7 and 14 d, whereas low glucose levels promoted their expression.

Western blot analysis was used to examine the expression of the senescence-related protein p21 in SHED (Fig. 2E) and hBMSC (Fig. 2F). After 14 d, the high-glucose group showed reduced p21 expression in SHED ($p = 0.0018$) but increased p21 expression in hBMSC ($p = 0.0001$), when compared to the respective normal glucose group.

3.3. SHED are more dependent on glycolysis than hBMSC

To investigate the glucose metabolism of the two cell types, we measured their glucose consumption (Fig. 3A) and lactic acid production (Fig. 3B) in the supernatant of the culture medium at 0, 12, 24, and

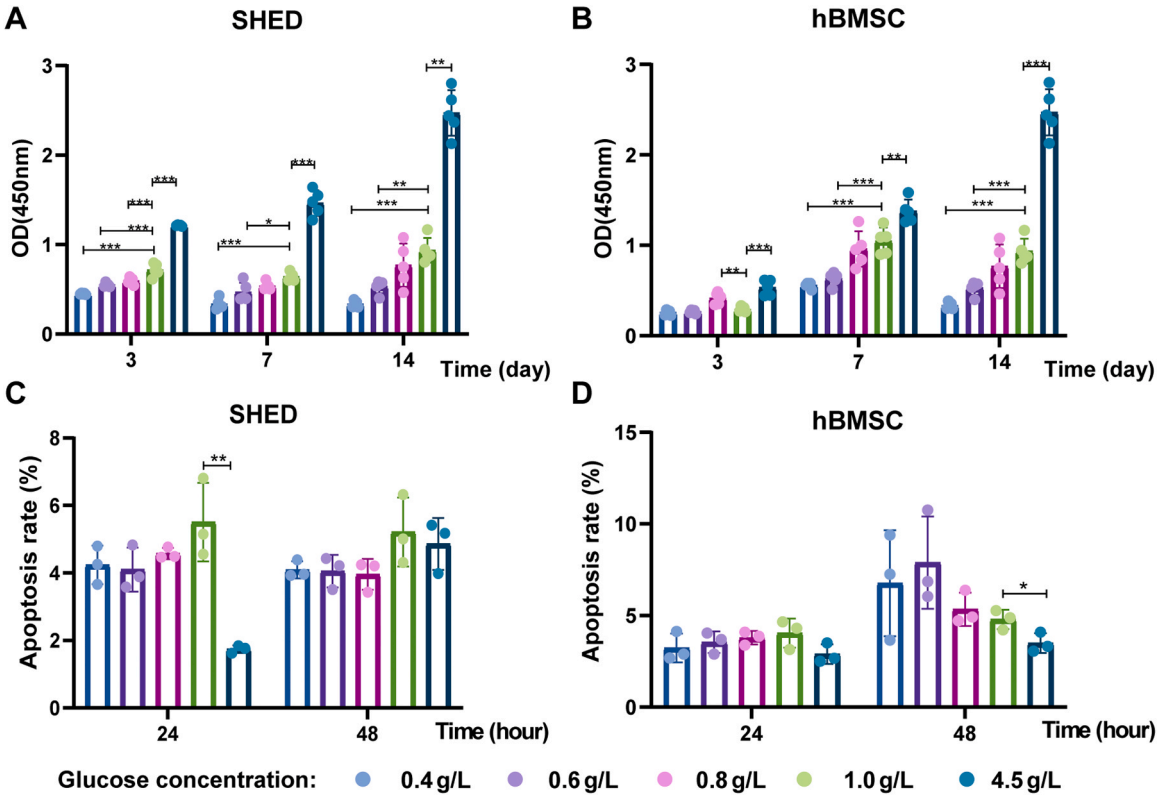

Fig. 1. Proliferation and apoptosis of stem cells from human exfoliated deciduous teeth (SHED) and human bone marrow-derived mesenchymal stem cells (hBMSC) depends on the concentration of glucose. Proliferation of SHED (A) and hBMSC (B) following incubation with the indicated concentrations of glucose for 3, 7, or 14 d. Apoptosis of SHED (C) and hBMSC (D) following incubation with the indicated concentrations of glucose for 24 h and 48 h. The normal glucose group served as the control. * $p < 0.05$, * * $p < 0.01$, and * ** $p < 0.001$.

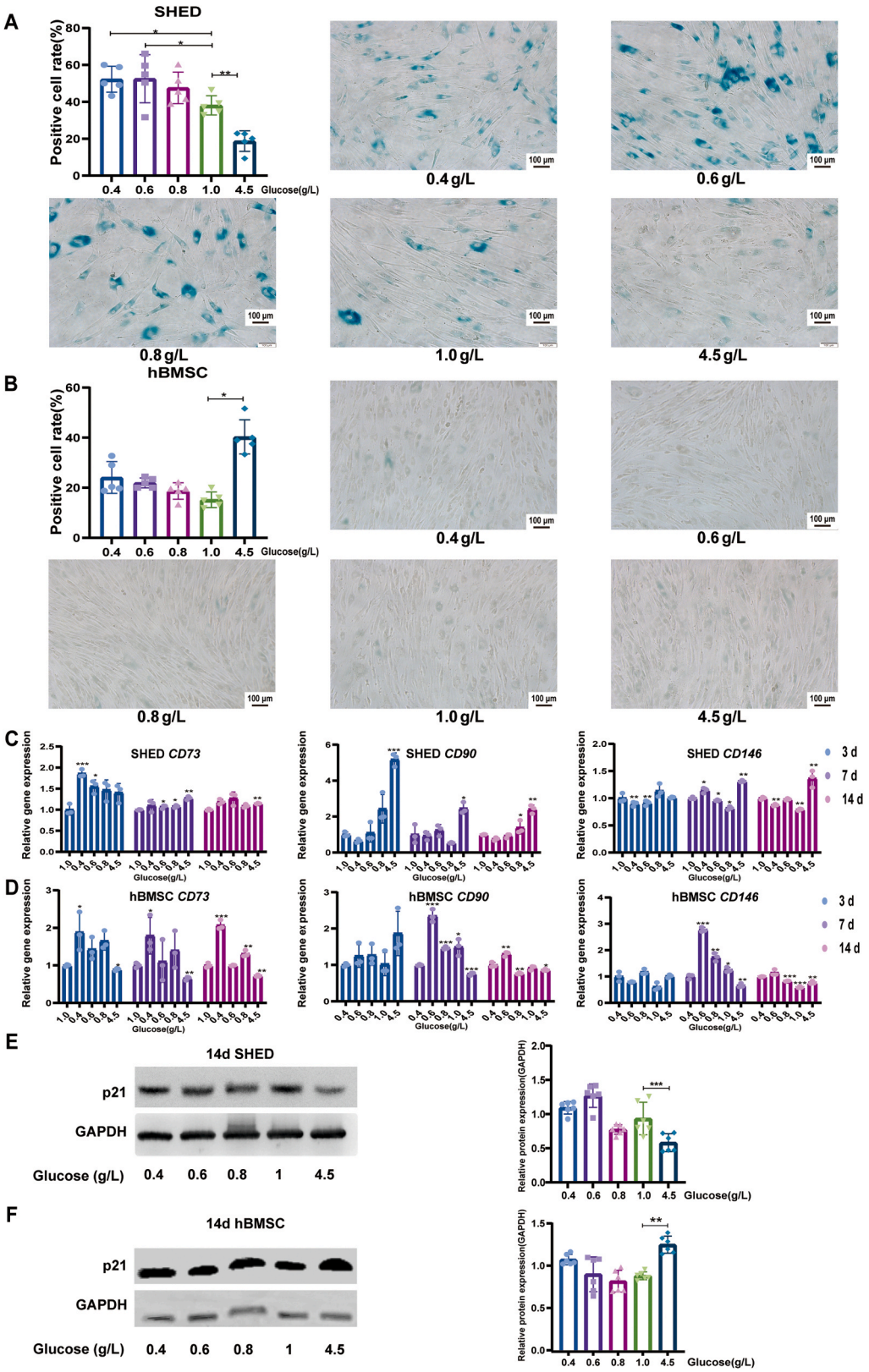

Fig. 2. Effects of varying glucose concentrations on senescence and stemness of stem cells from human exfoliated deciduous teeth (SHED) and human bone marrow-derived mesenchymal stem cells (hBMSC). Senescence-associated β-galactosidase activity staining of SHED (A) and hBMSC (B) were measured after 14 d of culture at the indicated glucose concentration. Representative images are shown. mRNA levels of *CD73*, *CD90*, and *CD146* in SHED (C) and hBMSC (D) were measured after culture for 3, 7, or 14 d at the indicated glucose concentrations. Glyceraldehyde 3-phosphate dehydrogenase (GAPDH) mRNA expression served as a loading control. Expression of the senescence-associated protein p21 in SHED (E) and hBMSC (F) following culture in the indicated concentrations of glucose for 14 d. GAPDH protein served as a loading control. Representative western blot images and averaged changes shown. * $p < 0.05$, * * $p < 0.01$, and * ** $p < 0.001$ vs. normal glucose group.

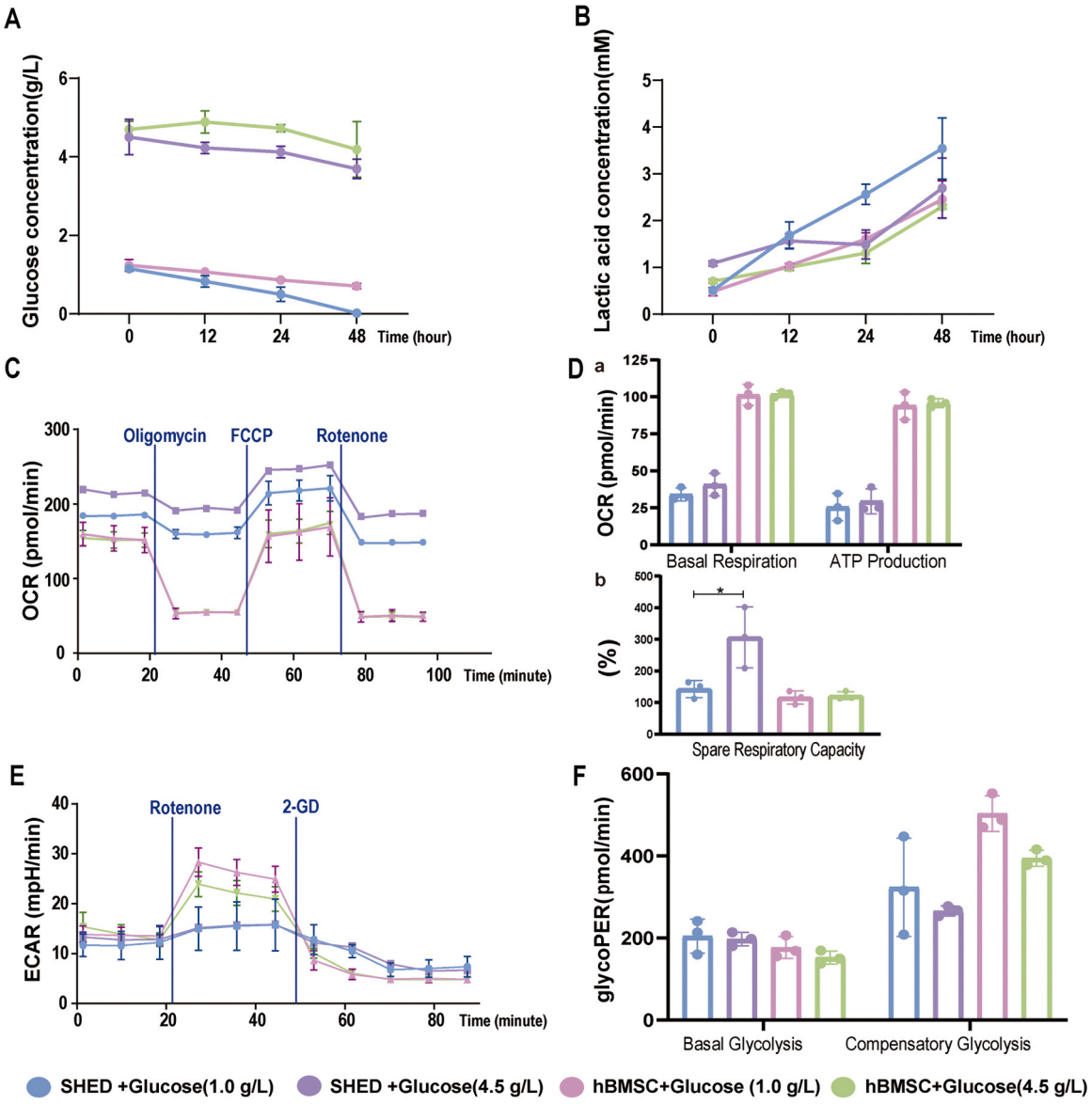

Fig. 3. Oxidative phosphorylation and glycolytic rate in stem cells from human exfoliated deciduous teeth (SHED) and human bone marrow-derived mesenchymal stem cells (hBMSC) cultured in high and normal glucose cooncentrations. Glucose consumption (A) and lactic acid production (B) in SHED and hBMSC at the indicated concentrations of glucose. (C) Oxygen consumption rate (OCR) in SHED and hBMSC following the addition of either oligomycin, carbonyl cyanide-4-(trifluoromethoxy) phenylhydrazone (FCCP), or 2-deoxy-D-glucose (2-DG). (D) Basal respiration, ATP production (a)and spare respiration capacity (b) in SHED and hBMSC in high or normal glucose concentrations. (E) extracellular acidification rate (ECAR) following addition of rotenone and 2-DG in SHED and hBMSC cultured in high or low glucose concentrations. (F) Basal and compensatory glycolysis capacity in SHED and hBMSC cultured in normal or high glucose concentrations.

48 h. Glucose consumption was higher in SHED than in hBMSC in both glucose groups (Fig. 3A), with SHED consuming almost all (98.34% ± 0.74%) glucose in the normal glucose medium by 48 h. With increased culture time, lactic acid production increased in both cell types, suggesting that a shared importance of glycolysis in energy production.

OXPHOS (Fig. 3C and D) and glycolysis (Fig. 3E and F) were detected in both cells at 24 h. Basal respiration and ATP production in hBMSC were significantly higher than those in SHED in the normal glucose and high glucose groups (Fig. 3D). High glucose levels increased the spare respiratory capacity of SHED ($p = 0.0195$) compared to the normal glucose group but had no effect on those of hBMSC between the normal glucose group and the high glucose group (Fig. 3D). Therefore, compared with SHED, hBMSC have higher OXPHOS activity and potentially produce more ATP either in the normal glucose group or the high glucose group. Basal and compensatory glycolysis in SHED did not differ between high and normal glucose levels (Fig. 3F). Compared with hBMSC, the basic glycolytic flux of SHED was higher, but the compensatory glycolysis of SHED was weaker either in the normal glucose group or the high glucose group. High glucose levels compromised the compensatory glycolytic ability of hBMSC compared to the normal glucose level, suggesting that glycolysis contributes more to energy supply in SHED than in hBMSC.

3.4. High glucose concentration inhibits SHED senescence by inhibiting autophagy

To explore the mechanistic differences in glucose metabolism between SHED and hBMSC, we studied metabolism-related autophagy proteins LC3B and p62 and their upstream regulation by the AMPK

signaling pathway (Fig. 4). Comparing to the normal glucose group, SHED in the high glucose group showed significantly lower expression of p21 ($p = 0.0001$), the autophagy-related proteins LC3II/LC3I ($p = 0.0215$), and p62 ($p = 0.0003$) than in the normal glucose group, indicating that autophagy was reduced. Additionally, the expression of p-AMPK/AMPK was lower in the high glucose group than in the normal glucose group, suggesting activation of the AMPK signaling pathway. Rapamycin was used as an activator of autophagy for comparison. Compared to the untreated the high glucose groups, the levels of LC3II/LC3I ($p = 0.0409$) and p62 ($p = 0.0046$) was significantly higher in the high-glucose group treated with rapamycin (Fig. 4), indicating that autophagy was activated. In addition, the level of senescence-related protein p21 was significantly higher in the high-glucose group treated with rapamycin ($p = 0.0053$) than in the untreated high-glucose group (Fig. 4). In contrast, there was no difference in p21 expression in the normal glucose group with or without rapamycin.

4. Discussion

Several major drawbacks to using hBMSC in regenerative medicine include the challenge to obtain sufficient nucleated cells and decreased therapeutic potential with age (Salazar-Noratto et al., 2020; Stolzing, Jones, McGonagle, & Scutt, 2008). Therefore, there is strong interest in the identification of alternative stem cell sources for regenerative medicine. One potential source is SHED; these possess the highest concentration of mesenchymal cells. Modulation of the SHED local microenvironment, such as glucose concentration, could be used to regulate cell behavior to better understand their function and improve their in vivo therapeutic use (Kichenbrand et al., 2020). Therefore, we compared SHED and hBMSC under different glucose concentrations and assessed how glucose influenced cell proliferation, viability, and senescence. Previous studies have recommended 1 g/L glucose to cultivate hBMSC in vitro (Kemp, Hows, & Donaldson, 2005) and have reported that 4.5 g/L glucose promotes hBMSC proliferation and reproductive senescence (Chang et al., 2015; Ryu et al., 2010), which is consistent with our results. High glucose levels enhanced SHED proliferation but, in contrast to our expectations, inhibited their senescence. Thus, we speculated that the distinct response of SHED and hBMSC senescence to glucose changes might be attributed to glycometabolic differences.

Glycolysis and OXPHOS are the two major cell energy-generating pathways. Glycolysis is the preferred metabolic pathway for stem cell self-renewal and proliferation, while the transition from glycolysis to mitochondrial OXPHOS is critical for stem cell differentiation (Folmes, Dzeja, Nelson, & Terzic, 2012). When stem cells enter the proliferative phase, glycolysis provides energy and macromolecules via the pentose phosphate pathway (Lunt & Vander Heiden, 2011; Ly, Lynch, & Ryall, 2020). In our study, the cumulative increase in lactic acid production over 48 h indicated that glycolysis was the major cell energy contributor for both cell types. We used the seahorse extracellular flux analyzer to measure the in vitro oxygen consumption rate and extracellular acidification rate, thereby determining both OXPHOS and glycolysis (van der Windt, Chang, & Pearce, 2016); hBMSC exhibited high OXPHOS, whereas SHED exhibited high glycolysis. One glucose molecule can generate 30–32 molecules of ATP via OXPHOS, whereas glycolysis only generates two. This difference in ATP generation explains why the ATP yield of hBMSC was significantly higher than that of SHED. Spare respiratory capacity was also used to assess the ability of cells to respond to energy metabolism challenges and, by extension, their adaptability in response to environmental changes. High glucose levels improved spare respiratory capacity of SHED, demonstrating that high glucose levels improved the flexibility of SHED glucose metabolism. The mitochondrial inhibitors Rot/AA effectively inhibited OXPHOS, prompting hBMSC to utilize glycolysis to satisfy their energy needs. This explains why compensatory glycolysis was significantly higher in hBMSC than in SHED. In addition, compared with normal glucose levels, high levels of glucose impaired the compensatory glycolytic capacity of hBMSC. This result indicates that SHED performed better in a high-glucose culture, whereas hBMSC performed better in a normal glucose culture. An increasing number of studies have shown that the proliferation ability of SHED is significantly higher than that of hBMSC at 1 g/ L concentration of glucose (Kunimatsu et al., 2018). Given the high glycolytic activity of SHED, this suggests that SHED are more “naïve” stem cells than hBMSC.

Autophagy has a strong influence on cell stemness and senescence (García-Prat, Martínez-Vicente, & Muñoz-Cánoves, 2016). Appropriate autophagy can promote cell metabolism and maintain stemness, but excessive autophagy can cause cell senescence or death (García-Prat, Martínez-Vicente & Perdiguero, Ortet et al., 2016), which is consistent with our results. Since SHED adopted glycolysis to supply energy, they required higher amounts of glucose than hBMSC. SHED cultured under normal glucose conditions may be in a “glucose-deficient” state, while high glucose levels appear to favor growth and maintain physiological autophagy levels and a well-balanced metabolic state. This suggestion is supported by the fact that normal glucose levels activated the SHED AMPK signaling pathway, a key pathway for catabolism. After treatment with the autophagy activator rapamycin, the normal metabolic state of

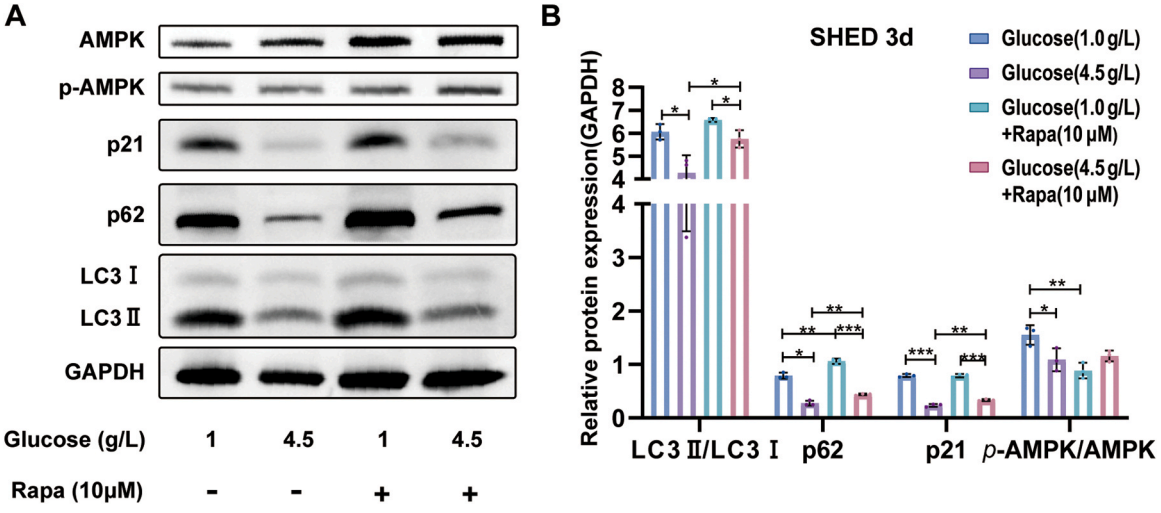

Fig. 4. Glucose concentration alters autophagy and adenosine 5′-monophosphate protein kinase alpha 1 activation in stem cells from human exfoliated deciduous teeth (SHED). Glyceraldehyde 3-phosphate dehydrogenase (GAPDH) protein expression served as a loading control. * $p < 0.05$, * * $p < 0.01$, and * ** $p < 0.001$ vs. the normal glucose group.

SHED was disrupted and autophagy increased, thus causing cell senescence. SHED cultured under normal glucose concentrations exhibited high autophagy levels because of "low glucose" starvation. We inferred that treatment with autophagy activators resulted in a large, irreversible increase in cell senescence in SHED, despite increased autophagy.

In conclusion, we demonstrated that hBMSC and SHED have different glucose metabolism phenotypes. Specifically, SHED are more suitable for culture in a high glucose condition, whereas a normal glucose condition is preferable for hBMSC However, our work has not established evidence of the expression levels of key enzymes and their enzyme activities of glucose metabolism. Additionally, high glucose concentration was defined as 4.5 g/L without further subdivision. Hence, it will be necessary for future studies to further refine the levels of a high glucose concentration. Lastly, we identified reduced autophagy as the cellular mechanism whereby high glucose reduces SHED senescence. If regulation and control of the stem cell behavior is to be realized, the upstream and downstream signal pathways of autophagy will need to be further explored. This finding highlights the benefit of culturing SHED under high glucose concentrations.

Funding statement

This study was funded by the Beijing Natural Science Foundation (Grant number: 7222222) and Peking University Medicine Fund of Fostering Young Scholars' Scientific & Technological Innovation (BMU2022PY021).

CRediT authorship contribution statement

Jinjin Lu: Conceptualization, Methodology, Investigation, Resources, Writing – original draft. **Lixin Zhang:** Methodology. **Ningxin Zhu:** Conceptualization, Writing – original draft. **Fei Xie:** Conceptualization, Re- sources, Writing – original draft. **Man Qin:** Conceptualization, Visualization, Writing – review & editing. **Yuanyuan Wang:** Conceptualization, Writing – review & editing, Funding acquisition. All of the authors approved of the version to be submitted.

Data Availability

Data are available from the authors upon request.

Acknowledgements

This experiment was completed during a severe wave of COVID-19. I would like to thank Professor Niu Yan from Peking University College of Pharmacy and the teachers from the Animal Laboratory of Peking University College of Stomatology for helping us going through this tough times.

Conflicts of interest

None.

References

Asghari, M., Nasoohi, N., & Hodjat, M. (2021). High glucose promotes the aging of human dental pulp cells through Wnt/beta-catenin signaling. *Dental and Medical Problems, 58*(1), 39–46.

Chang, T. C., Hsu, M. F., & Wu, K. K. (2015). High glucose induces bone marrow-derived mesenchymal stem cell senescence by upregulating autophagy. *PLoS One, 10*(5), Article e0126537.

Folmes, C. D., Dzeja, P. P., Nelson, T. J., & Terzic, A. (2012). Metabolic plasticity in stem cell homeostasis and differentiation. *Cell Stem Cell, 11*(5), 596–606.

García-Prat, L., Martínez-Vicente, M., & Muñoz-Cánoves, P. (2016). Autophagy: A decisive process for stemness. *Oncotarget, 7*(11), 12286–12288.

García-Prat, L., Martínez-Vicente, M., Perdiguero, E., Ortet, L., Rodríguez-Ubreva, J., Rebollo, E., & Muñoz-Cánoves, P. (2016). Autophagy maintains stemness by preventing senescence. *Nature, 529*(7584), 37–42.

Kemp, K. C., Hows, J., & Donaldson, C. (2005). Bone marrow-derived mesenchymal stem cells. *Leuk Lymphoma, 46*(11), 1531–1544.

Kichenbrand, C., Grossin, L., Menu, P., & Moby, V. (2020). Behaviour of human dental pulp stem cell in high glucose condition: Impact on proliferation and osteogenic differentiation. *Archives of Oral Biology, 118*, Article 104859.

Kim, H.J., Ji, B.R., Kim, J.S., Lee, H.N., Ha, D.H., & Kim, C.W. (2012). Proteomic analysis of proteins associated with cellular senescence by calorie restriction in mesenchymal stem cells. In Vitro Cell Dev Biol Anim, 48(3), 186–195.

Kunimatsu, R., Nakajima, K., Awada, T., Tsuka, Y., Abe, T., Ando, K., & Tanimoto, K. (2018). Comparative characterization of stem cells from human exfoliated deciduous teeth, dental pulp, and bone marrow-derived mesenchymal stem cells. *Biochemical and Biophysical Research Communications, 501*(1), 193–198.

Lunt, S. Y., & Vander Heiden, M. G. (2011). Aerobic glycolysis: meeting the metabolic requirements of cell proliferation. *Annual Review of Cell and Developmental Biology, 27*, 441–464.

Ly, C. H., Lynch, G. S., & Ryall, J. G. (2020). A metabolic roadmap for somatic stem cell fate. *Cell Metabolism, 31*(6), 1052–1067.

Miura, M., Gronthos, S., Zhao, M., Lu, B., Fisher, L. W., Robey, P. G., & Shi, S. (2003). SHED: stem cells from human exfoliated deciduous teeth. *Proceedings of the National Academy of SciencesUnited States A, 100*(10), 5807–5812.

Ryu, J. M., Lee, M. Y., Yun, S. P., & Han, H. J. (2010). High glucose regulates cyclin D1/E of human mesenchymal stem cells through TGF-beta1 expression via Ca2+/PKC/MAPKs and PI3K/Akt/mTOR signal pathways. *Journal of Cellular Physiology, 224*(1), 59–70.

Sakaguchi, Y., Sekiya, I., Yagishita, K., & Muneta, T. (2005). Comparison of human stem cells derived from various mesenchymal tissues: Superiority of synovium as a cell source. *Arthritis and Rheuma, 52*(8), 2521–2529.

Salazar-Noratto, G. E., Luo, G., Denoeud, C., Padrona, M., Moya, A., Bensidhoum, M., & Petite, H. (2020). Understanding and leveraging cell metabolism to enhance mesenchymal stem cell transplantation survival in tissue engineering and regenerative medicine applications. *Stem Cells, 38*(1), 22–33.

Stolzing, A., Jones, E., McGonagle, D., & Scutt, A. (2008). Age-related changes in human bone marrow-derived mesenchymal stem cells: Consequences for cell therapies. *Mechanisms of Ageing and Development, 129*(3), 163–173.

van der Windt, G. J. W., Chang, C. H., & Pearce, E. L. (2016). Measuring bioenergetics in T cells using a seahorse extracellular flux analyzer. *Current Protocols in Immunology, 113*, 3.16b.11-13.16b.14.

Yoshimura, H., Muneta, T., Nimura, A., Yokoyama, A., Koga, H., & Sekiya, I. (2007). Comparison of rat mesenchymal stem cells derived from bone marrow, synovium, periosteum, adipose tissue, and muscle. *Cell and Tissue Research, 327*(3), 449–462.

Zhang, N., Chen, B., Wang, W., Chen, C., Kang, J., Deng, S. Q., & Han, F. (2016). Isolation, characterization and multi-lineage differentiation of stem cells from human exfoliated deciduous teeth. *Molecular Medicine Reports, 14*(1), 95–102.